Analyses by Global-Local Method of Ultrasonic Guided Waves Propagation in Pristine and Defective Plates for Accurate Quantitative SHM

MARGHERITA CAPRIOTTI[1], MINGYUE ZHANG[1,2], LUIS ESCALONA[1], FRANCESCO LANZA DI SCALEA[2] and ANTONINO SPADA[3]

ABSTRACT

The efficient and accurate modeling of ultrasonic guided waves (UGWs) can be a very effective tool to optimize UGWs inspections and enable defect characterization when performing structural health monitoring (SHM). Among the several strategies, hybrid methods provide the capability of representing accurately the hosting structure and defect configurations, while leveraging the decreased computational costs of reduced-order and/or semi-analytical methods.

In this work, the Global-Local method is used to simulate UGW propagation in composite plates with defects, to study the effect of the incident mode interaction with the scatterer and its features (size, location, local zone relation). To do so, the evolution of the method is presented to account for the inclusion of evanescent modes and to accommodate the forced solution framework. In the first improvement, the role of evanescent modes will be discussed with respect to accuracy and computational cost considerations, providing guidelines for effective UGW modeling in composite materials. In the second upgrade, the 2D time-space response to different spatial and temporal sources is observed and analyzed in terms of its spectral content, to differentiate pristine and defective conditions, in composite materials with increasing defect severity. These improvements in the numerical framework of the Global-Local approach are significant to enable quantitative SHM and prognostics by accurate and efficient predictions of UGW scattered responses, and to advance defect characterization by UGWs by analyses of UGW data.

INTRODUCTION

In recent years, ultrasonic guided waves (UGWs) have been widely used in Non-destructive Evaluation (NDE) and Structural Health Monitoring (SHM) fields. Com-

[1]Department of Aerospace Engineering, San Diego State University, 5500 Campanile Drive, San Diego, CA 92182, USA.

[2]Department of Structural Engineering, University of California, San Diego, 5500 Campanile Drive, San Diego, CA 92182, USA.

[3]Department of Engineering, University of Palermo, V.le delle Scienze, Edificio 890128, Palermo, Italy

pared to traditional ultrasonic wave testing, UGWs offer large-area inspection and deep penetration. Analytical methods to calculate guided wave propagation solutions have been developed and applied to multi-layered structures, e.g. the global matrix or transfer matrix method [1] [2]. However, purely theoretical solutions are limited to simple geometries and/or defect cases. For more general applications, several fully numerical or hybrid methods have been employed to model UGWs propagation.

Although finite element methods (FEM) are still the most widely used numerical strategy for solving problems of wave propagation, the utilization of full FE discretization can be computationally demanding and inefficient, particularly for simulating the inspection of large waveguides and scattering over broad or multiple frequency ranges. On the contrary, hybrid methods offer an efficient and accurate compromise, since they combine known analytical solutions to describe the wave propagation in the global structure and numerical solutions to efficiently simulate UGWs interaction with discontinuities within the local region. Among the hybrid methods, the Global-Local (GL) method, a hybrid Semi-analytical Finite Element (SAFE)-FE method has been proposed [3] and developed for quantitative NDE in 2D [4] and 3D [5] multilayered structures with defects.

Furthermore, the existence of propagating and non-propagating modes adds to the complexity of UGW scattering. This aspect is especially significant when the contribution of near-field effects, in the vicinity of a defect or geometrical discontinuity, cannot be disregarded. SAFE methods have been used to model wave propagation in damped and undamped waveguides of isotropic and composite materials of arbitrary cross-section, including analysis of evanescent modes [6]. A hybrid Wave Finite Element (WFE)/FE method was used to study the effect of defect size on UGWs scattering by a local defect in the structural waveguide, including evanescent modes and a forced formulation to compute time-domain scattered waveform [7]. In this work, the GL method is used to study the role of evanescent modes in the accurate modeling of UGW propagation in isotropic and composite plate waveguides, with respect to features of the defect in relation to the local zone.

Despite significant progress in computer engineering, the primary constraint of such algorithms lies in their computational expenses. The authors are endeavoring to reduce the impact of the numerical solution. A code parallelization has been implemented, and results in terms of computational gain and speedup are presented in [8]. Moreover, the formulation has been extended with subroutines that enable forced response analysis [8]. This formulation enables to compute the transient response resulting from UGW scattering of an incident wave with any discontinuity. The response can be extracted in a pitch-catch mode and across a wide frequency range to allow for UGW virtual inspections and analyses.

THEORETICAL FORMULATION

Let us consider the general 2D scattering problem shown in Figure 1. The GL method formulates the UGW propagation problem by separating the complex waveguide into two regions. A detailed formulation can be found in [4]. An incident time harmonic guided wave excited in the global region travels along the propagation direction and is

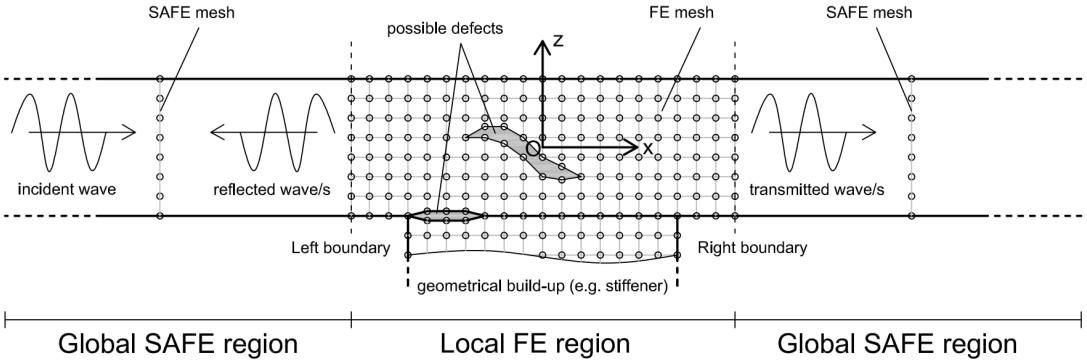

Figure 1. Geometrical representation of the scattering of an incident wave in reflected and transmitted waves from a local region, with indication of the adopted discretization strategies in each region of the Global-Local approach.

scattered into reflected and transmitted waves, after interacting with the discontinuity within the local region.

Defining the vector U^g for the nodal displacements, K^g for the stiffness matrix, M^g for the mass matrix, and F^g for the force vector obtained in the global region, the dynamic undamped equilibrium equation is obtained as:

$$(K^g - \omega^2 M^g)U^g = F^g \tag{1}$$

where in the case of an unforced solution, the right side of Eq. 1 is 0. This constitutes a generalized eigenvalue problem where wavenumbers ξ and wavemodes Φ can be found in terms of eigenvalues and eigenvectors. The eigenvalues occur as pairs of real numbers $(\pm\xi_{Re})$, representing propagating waves in the $\pm x$ directions, as pairs of complex conjugate numbers $(\pm\xi_{Re} \pm i\xi_{Im})$, representing evanescent waves decaying in the $\pm x$ directions, or as pairs of purely imaginary numbers $(\pm i\xi_{Im})$, representing the nonoscillating evanescent waves in the $\pm x$ directions.

Following [9] and [10], the dispersion curves are built calculating the associated phase (C_p) and group (C_g) velocities, including attenuation and energy velocity.

Attenuation and energy velocity are obtained as follows:

$$att = \xi_{Im} \tag{2}$$

$$c_{En} = \frac{\frac{1}{\Gamma}\int_\Gamma \boldsymbol{P}\cdot\boldsymbol{n}d\Gamma}{\frac{1}{T}\int_T(\frac{1}{\Gamma}\int_\Gamma e_{tot}d\Gamma)dt} \tag{3}$$

where Γ is the cross-sectional area, $\boldsymbol{P}$ is the Poynting vector (real part only), n is the propagation direction unit vector, e_{tot} is the total energy density, T is the period.

The energy is calculated as Eq. 4, for each scattered mode.

$$E^j = -\frac{|A_j|^2}{2} Re\left[i\omega \boldsymbol{F}^{j^T}\bar{\boldsymbol{\Phi}}^j\right] \tag{4}$$

where A_j are the scattering coefficients, and $\boldsymbol{F}^j$ and $\boldsymbol{\Phi}^j$ are the consistent forces and corresponding mode shapes for mode j.

The scattering spectra can be obtained from the conversation of energy verified between the incident and the scattered modes:

$$E_{in} = \sum_{j=1}^{N_M} (E_{Refl}^{(j)} + E_{Transm}^{(j)}) \tag{5}$$

NUMERICAL INVESTIGATIONS

Evanescent Modes

The Global-Local Matlab code developed by [4] was improved to include evanescent modes in the analysis [10]. A series of numerical analyses were conducted on composite plates with defects, to study the accuracy of the numerical solution. The composite plates had a 10-layer layup $[0/+45/+90/-45/0]_S$ of T800/3900-2 Graphite/Epoxy unidirectional laminate, with a thickness of 0.2 mm for each layer. Material properties were those used in [11] and reported in Table I in the principle direction of material symmetry, where 1 represents the fiber direction, 2 represents the direction perpendicular to the fibers in the lamina plane, and 3 represents the through-thickness direction. The density of each lamina was $1550kg/m^3$. Throughout the tests conducted, the thickness of the plates was fixed as 2mm, while a length of 5mm was chosen as the size of the local region for most of the cases, and varied in some cases. The geometry, size, and location of the defect varied inside the local region across different tests.

To ensure numerical accuracy, 20 finite elements per wavelength were used. Accordingly, each finite element was selected to be linear (four Gauss points) and squared in shape, with sides equal to 0.1mm. At each frequency, the eigenvalue problem returns a number of evanescent modes. They were selected on the value of $abs(Im(\xi h)$ with respect to a threshold value since higher order evanescent modes are found to have negligible effect in the analysis.

In Figure 2 the results of an S0 incoming mode traveling through the defected composite plate are reported. The geometrical representation of the plate is shown in Figure 2 a, the rectangular notch has a length of 2 mm and a depth of 1 mm, and is located at a distance of 1.5 mm from the local zone (LZ) boundaries. In Figure 2b a numerical error is observed on the total scattered energy in the absence of evanescent modes with a maximum error of 18%. On the contrary, when evanescent modes are included (Figure 2c), the errors are effectively corrected. It is important to note that the scattered energy of each mode is also corrected.

Parallelization Computing

This section presents the speedup analysis of the serial implementation [8]. The serial GL method computes the solutions for each frequency sequentially. The optimized

TABLE I. ELASTIC PROPERTIES OF THE COMPOSITE LAMINA

Property	C_{11}	C_{12}	C_{13}	C_{22}	C_{23}	C_{33}	C_{44}	C_{55}	C_{66}
GPa	162	3.98	3.98	10.4	3.81	10.4	3.45	6.21	6.21

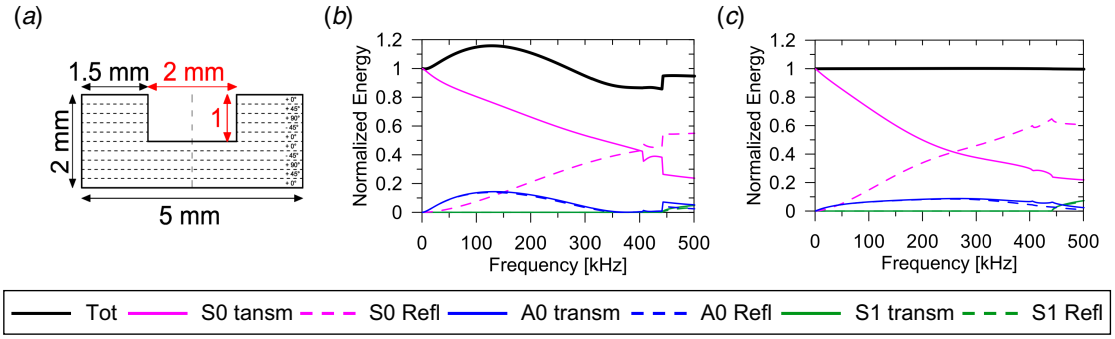

Figure 2. S0 incident energy spectra for a composite plate with a 2 × 1 mm rectangular notch (LZS = 5 mm): a) geometry of the plate; b) solutions without evanescent modes; c) solutions with evanescent modes.

version solves the coupled solution in parallel, where each branch executes a different frequency. The scalability of the code is influenced by both the number of frequencies to analyze and the local region size. The former is related to the number of parallel processors used when branches are running simultaneously, while the latter is related to the amount of memory required per branch. The problem size is determined by the finite element size.

An 8-ply carbon-fiber reinforced polymer (CFRP) plate with a length of 1 cm and a thickness of 1 mm was tested. Material properties were those used in [3]. The element thickness dz is determined by $dz = h \times \frac{t_z/n_p}{2}$. In this equation, t_z is the plate thickness, n_p is the number of plies, and h is the scaling factor used for mesh refinement. The element length dx is given by $dx = h \times \frac{\lambda}{\beta}$, where the scaling factor h is also used, and a factor β of 10 is used to guarantee at least 10 elements per wavelength. In this work, four element sizes were tested including $2h$, h, $h/2$, and $h/4$.

The GL code was tested for the different problem sizes on a workstation with processor Intel® Xeon® W-2255 CPU @3.70 GHz, 10 physical cores, 20 logical processors, and 31.7 GB of RAM memory. The Matlab code was implemented using the parallel computing toolbox.

Speedup was tested for 1, 2, 4, 8, and 16 workers. Figure 3 shows the effect of the number of workers for different problem sizes on the CFRP plate. For all problem sizes, the computational time decreases as the number of workers increases up to the number of physical cores available. However, when the number of workers is greater than the number of cores but less than the number of logical processors, there is a minor reduction or increase in execution times.

RESULTS AND DISCUSSION

Unforced Solution with Evanescent Modes

To develop some general guidelines or rules of thumb, a comprehensive parametric analysis was conducted for composite plates with a notch. Various tests were performed, with a focus on varying the distance between LZ and the scatterer, and the scatterer

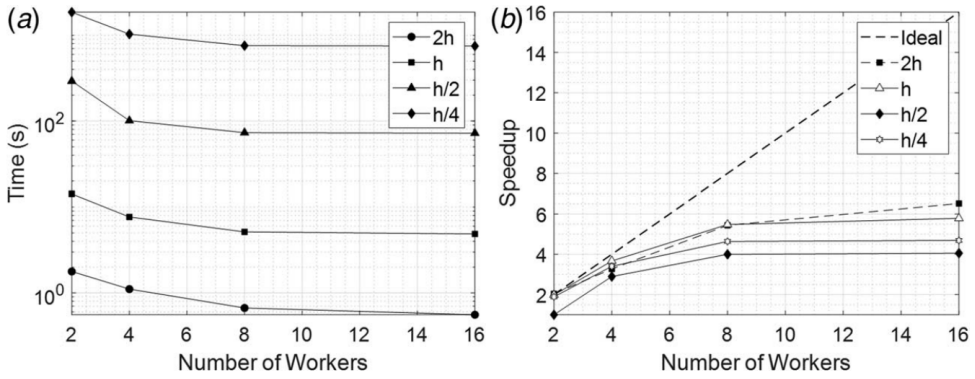

Figure 3. Effect of parallel computing for different problem sizes on the CFRP plate case: a) computational time versus the number of workers; b) speedup versus the number of workers.

dimensions. The results of the analysis are presented in terms of the overall error in the total normalized energy. This error parameter is defined as the cumulative error over the entire frequency range and is determined by comparing the area under the numerically calculated effective curve with the expected value of one:

$$E_{rr} = \sum_{k=1}^{n_f} \frac{|S_{num}^k - S_{exp}^k|}{S_{exp}^k} \tag{6}$$

where n_f is the total number of frequency steps, S_{num}^k is the effective observed numerical area under the total normalized energy curve, and S_{exp}^k is the expected area.

Figure 4 presents the results of the parametric analysis performed on the composite plate. In Figure 4a, the size of LZ is set to 5 mm, and the rectangular notch at the top of the plate has an aspect ratio of 2. The depth of the notch is varied from 0.2

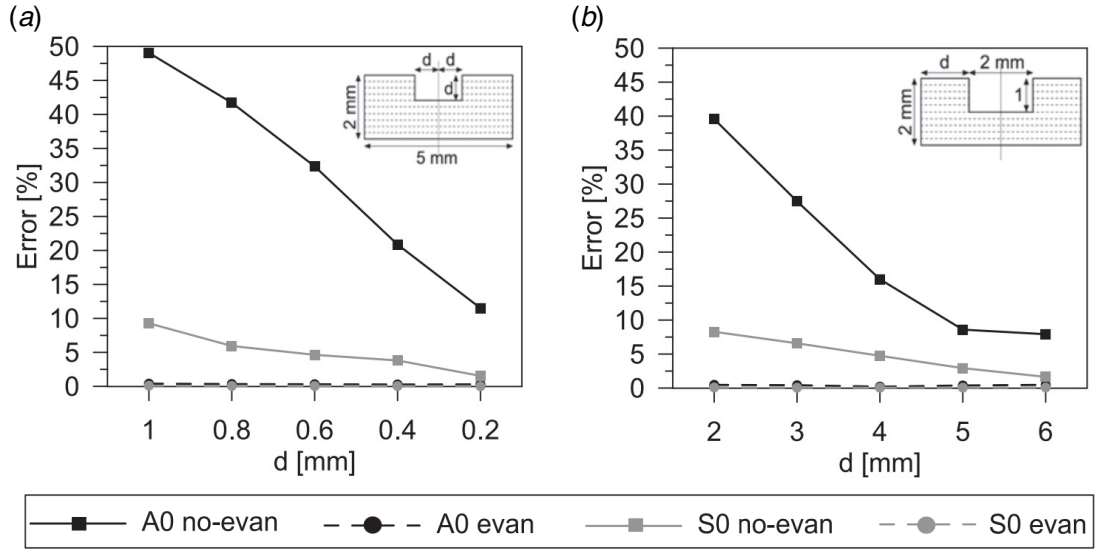

Figure 4. Parametric analysis for a composite plate in terms of total normalized energy error in the case of a) size of a rectangular notch (LZS = 5 mm); b) distance from the left boundary, for a 2 $\times$ 1 mm rectangular notch (varying LZS).

mm to 1mm. In Figure 4b, the width and the depth of the notch are set to 2 mm and 1 mm, while the distance between the LZ boundary and notch ranges from 2 mm to 6 mm. When evanescent modes were not considered, errors were generally higher for both A0 and S0 incoming modes. It is also evident that higher errors were obtained for the A0 mode compared to the S0 mode. When the S0 mode is incoming and evanescent modes are not considered, it was found that a rectangular notch with an aspect ratio of 2 was acceptable if its depth did not exceed 0.6 mm when the LZ was 5 mm wide. Alternatively, a minimum distance of 4 mm from the left boundary was necessary to achieve low errors. However, with an A0 incoming mode and no evanescent modes, a wider distance between the LZ and the scattered or a shallower depth is required. When evanescent modes are included, errors obtained from both incoming modes were less than 1%.

Forced Solution without Evanescent Modes

The forced solution was applied to the same 10-ply CFRP plates in a pristine and a notched configuration. The excitation used is a pure mode (quasi-S0), with a temporal function of a narrowband tone-burst at 150 kHz, duration of five cycles. The source is positioned at 0.01 m on the left of the origin, and receiver 1 is located at 0.1 m on the right. The displacements are presented in 2D over a grid of one hundred equally spaced receivers spaced by 1 mm. The solution is obtained for the frequency range (DC-801 kHz) with a frequency step of 2 kHz and time resolution of 0.62 μs.

The comparison of the resulting displacements between the pristine and 4-ply notched (d = 0.8mm) CFRP plate is illustrated in Figure 5. In Figure 5a, the displacement for the pristine plate shows wave propagation of the excited quasi-S0 mode. In contrast, the notched Figure 5b, causes mode conversion into a slower and more dispersive mode (quasi-A0), due to the defect's asymmetry. The scattered mode in transmission is particularly visible in the out-of-plane displacement and was expected as the scattering spectra in Figure 2c predicted.

CONCLUDING REMARKS

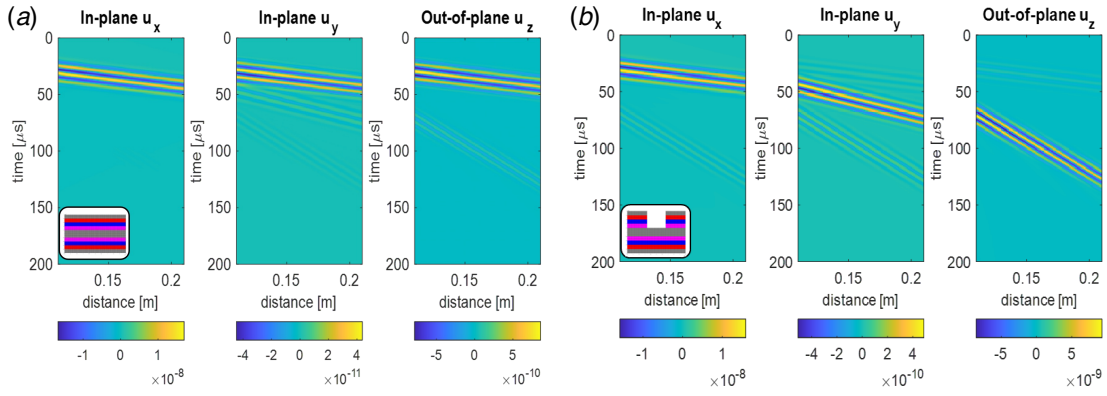

Figure 5. 2D spatiotemporal response of transmitted u_x, u_y, and u_z displacements for a quasi-S0 mode incident, 150 kHz, in a) pristine and b) 4-ply notched CFRP plates.

This work has presented the numerical framework and implementation of the improved Global-local method, highlighting its ability to effectively include evanescent modes in the analysis and adapt to the forced solution framework. The effect of evanescent modes has been studied by varying the size of the defect and the distance between the LZ and the scatterer. The requirement of ensuring a minimum distance between the LZ and the scatterer, based on the defect size and plate thickness, was found to be critical in the absence of evanescent modes. However, considering the evanescent modes can significantly reduce the numerical errors and, consequently, the required minimum distance. This leads to a reduction in computing costs while maintaining accurate results.

The inclusion of the forced solution utilizes normal mode expansion and enables the computation of the waveguide response, in either pristine or damaged state, at any location along the wave propagation direction and through the thickness. Additionally, it can calculate the response to any spatial and temporal forcing function applied through the thickness of the waveguide. Parallel computing is crucial for achieving accurate and efficient resolution of the forced solution.

In future work, exploring the selection of specific evanescent modes based on different scatterer and material properties can enhance accuracy and efficiency. Additional efforts, including experimental or numerical validations, can further validate the applicability of the method. The authors are currently improving the solution to address these limitations for quantitative non-destructive evaluation.

REFERENCES

1. Lowe, M. J. 1995. "Matrix techniques for modeling ultrasonic waves in multilayered media," *IEEE transactions on ultrasonics, ferroelectrics, and frequency control*, 42(4):525–542.
2. Rose, J. L. 2014. *Ultrasonic guided waves in solid media*, Cambridge University Press.
3. Srivastava, A. and F. Lanza di Scalea. 2010. "Quantitative structural health monitoring by ultrasonic guided waves," *Journal of Engineering mechanics*, 136(8):937–944.
4. Spada, A., M. Capriotti, and F. L. di Scalea. 2020. "Global-Local model for guided wave scattering problems with application to defect characterization in built-up composite structures," *International Journal of Solids and Structures*, 182:267–280.
5. Spada, A., M. Capriotti, and F. Lanza di Scalea. 2022. "Global–local model for three-dimensional guided wave scattering with application to rail flaw detection," *Structural Health Monitoring*, 21(2):370–386.
6. Bartoli, I., A. Marzani, F. L. Di Scalea, and E. Viola. 2006. "Modeling wave propagation in damped waveguides of arbitrary cross-section," *Journal of sound and vibration*, 295(3-5):685–707.
7. Zhou, W. and M. Ichchou. 2011. "Wave scattering by local defect in structural waveguide through wave finite element method," *Structural Health Monitoring*, 10(4):335–349.
8. Capriotti, M., L. Escalona, A. Spada, et al. 2022. "Improved Global-Local method for ultrasonic guided wave scattering predictions in composite waveguides and defects," in *ASME J Nondestructive Evaluation*, 6(4): 041003. doi: https://doi.org/10.1115/1.4056897.
9. Benmeddour, F., F. Treyssède, and L. Laguerre. 2011. "Numerical modeling of guided wave interaction with non-axisymmetric cracks in elastic cylinders," *International journal of Solids and Structures*, 48(5):764–774.
10. Spada, A., M. Zhang, F. Lanza di Scalea, and M. Capriotti. 2023. "The role of evanescent modes in global-local analysis of ultrasonic guided waves in plates with varying local zone-scatterer relations," *Journal of Vibration and Control*:10775463231168926.
11. Tong, L. and C. Soutis. 2013. *Recent advances in structural joints and repairs for composite materials*, Springer Science & Business Media.